Additional Thesis

The influence of spatial radar rainfall resolutions and land-use data on the urban water balance in Rotterdam

Anna Luisa Hemshorn de Sánchez

MSc. Water Management
Delft University of Technology
Faculty of Civil Engineering and Geosciences

Assessment Committee
Dr. ir. Marie-Claire ten Veldhuis, TU Delft
Dr. Marc Schleiss, TU Delft

The influence of spatial radar rainfall resolutions and land-use data on the urban water balance in Rotterdam

Anna Luisa Hemshorn de Sánchez

Abstract

While rainfall is the key input to most hydrological models, its precise characteristics are often uncertain. Runoff generation does not only depend on the measured rainfall resolution but also on the level of detail of land-use and therefore of the runoff generation. This study aims at identifying the influence of rainfall radar resolution and land-use data on the urban water balance in Rotterdam. Results show that the water balance in this study does not close properly, as more volume enters than leaves the system. This is most probably because infiltration is neglected and the reliability of the pumping data is uncertain. Furthermore, the Combined Sewer Overflow (CSO) volumes are overestimated which might be caused by the high uncertainty of the weir parameters and of the water levels at the non-monitored CSO weirs. This error multiplies with an increase in sewer district size, a higher amount of unmonitored CSOs and lower weir levels. When comparing the different resolutions, the water balance degrades remarkably with coarser land-use data detail and improves slightly with higher rainfall radar resolution, until reaching a certain threshold where the error is minimized. After this threshold the water balance closes less again. Possibly, the reduction in noise and in sensitivity to shifts in timing and location of the radar data with coarsening rainfall radar resolutions is responsible for these unexpected results. Furthermore, this study suggests that there might be a relationship between the changes in land-use resolution and the changes in rainfall radar resolution.

1. Introduction

Although rainfall is the key input to most hydrological models, accurate knowledge about its characteristics is often lacking (Segond, Wheater and Onof, 2007). Several studies have shown that a large portion of the hydrologic modeling errors is caused by uncertainties in rainfall estimates (Sun *et al.*, 2000; Kavetski, Kuczera and Franks, 2006; Moulin, Gaume and Obled, 2008; Mcmillan *et al.*, 2010). These uncertainties limit the accuracy of the models, reducing their value for operational use such as flood forecasting (Moulin, Gaume and Obled, 2008). This is especially relevant for urban catchments, as they are characterized by a high flood risk due to the reduced infiltration capacity of paved areas and the economic value of urban areas. Another important factor to consider in urban hydrological models is the impact of land-use on run-off generation, often described by the runoff coefficient. This coefficient not only depends on land-use but also on rainfall dynamics, spatial elevation and groundwater elevation (Yin *et al.*, 2017). Due to these dependencies, runoff coefficients are generally variable over time and thus difficult to determine.

1.1 Rainfall radar resolutions

To get further insight into the characteristics of rainfall, an appropriate measuring technique for this parameter has to be selected. Faures et al. 1995 cited in Bell and Moore (2000) found that even on a small scale of 4.4 ha a single rain gauge can lead to large uncertainties in the estimations of runoff. Furthermore, a rain gauge usually has a low spatial coverage and is therefore sensitive to spatial variability. In contrast, radar imagery has a high spatial coverage. For this reason, several authors (Bell and Moore, 2000; Einfalt *et al.*, 2004; Schellart, Shepherd and Saul, 2012) highlighted the importance of using radar imagery as a complement to rain gauge data. However, radar also has disadvantages and sources of errors. For instance, the spurious echoes resulting from buildings or trees and the refraction of the radar beam as it passes through air of varying densities can cause

errors (Schellart, Shepherd and Saul, 2012). Further examples include interferences with other electromagnetic radiation (especially in cities), non-meteorological targets such as planes, ships, birds and insects as well as the conversion from reflectivity to rain rate, which depends on drop size distribution. Nevertheless, for a specific time resolution there exists an optimum spatial resolution at which the error is minimized (Fabry *et al.*, 1994). An important aspect to consider is that the resolutions at which radar networks operate are often not high enough to meet the scale of urban hydrodynamics (Berne et al., 2004; Emmanual et al., 2012; Schellart, Sheperd and Saul, 2012 cited in Bruni *et al.*, 2015). On one hand, high resolutions are required for an appropriate representation of the hydrological response of urban systems. But these also imply additional strain on limited resources (e.g. calculation times) (Ochoa-Rodriguez *et al.*, 2015). For higher precipitation intensities, the accuracy of high-resolution rainfall estimates diminishes, which leads to a trade-off between high-resolution data and data accuracy (Van de Beek et al., 2010, Leijnse et al., 2010 cited in Ten Veldhuis and Olsen, 2012).

Several model-based studies were conducted aiming at determining critical thresholds for spatial but also temporal rainfall radar resolutions. Notaro *et al*. 2013 cited in Ochoa-Rodriguez *et al.* (2015) conducted a study based on a semi-distributed model for an area of 700 ha in Italy. They found that a spatial resolution of 1.7 km and a temporal resolution of 5 min were appropriate. Similarly, Gires et al. (2012) and Wang et al. (2012) cited in Ochoa-Rodriguez *et al.* (2015) used a semi-distributed model for London and proposed resolutions of 1 km and 5 min. Ochoa-Rodriguez *et al.* (2015) analyzed a large number of storms and a wide variety of urban catchments in North-West Europe as part of the RAINGAIN[1] project. Critical rainfall radar resolutions at which the response could be described properly were found by using semi-distributed hydrodynamic models. Results showed that the temporal resolution should be below 5 min, which is not met by regular national weather radars (5-10 min). The spatial resolution should be at sub-kilometric scales. For drainage areas below 1 ha, the input resolution should be at 100 m whereas a resolution of 500 m resulted to be enough for drainage areas between 1 ha and 100 ha. Larger areas only required a resolution of 1 km as long as the temporal resolution was smaller than 5 min. The study found that the effect of differences in resolution diminishes with increasing catchment drainage area. Ochoa-Rodriguez *et al.* (2015) found that hydrodynamic modeling results are more sensitive to variations in temporal resolution than in spatial resolution of rainfall input. The study revealed a strong interaction between the temporal and the spatial resolution. Furthermore, it suggested prioritizing improvements in temporal resolution while keeping in mind that both resolutions affect each other.

The downside of model-based research is that the model sensitivity to rainfall input resolution is also affected by other sources of uncertainty such as the estimation of parameters, model structure and characteristics like the slope, the degree of imperviousness or the presence of control elements (Bruni *et al.*, 2015). Higher-resolution fully-distributed models based on high resolution datasets, have a higher probability of being more sensitive to spatial resolution of rainfall input (Bárdossy and Das, 2006) and may therefore require rain resolutions smaller than 1 km (Schertzer et al., 2010; Gires et al., 2014a,b; Pina and Ochoa-Rodriguez, 2014; Ichiba et al., 2015 cited in Ochoa-Rodriguez et al., 2015).

Far fewer studies were conducted based on field observations instead of model-based sensitivity analysis. Berne *et al.* (2004) related lag time to the spatial scales of urbanized catchments and found differing required temporal and spatial resolutions depending on the catchment size. For catchments in the order of 1000 ha, resolutions of 5 min and 3 km are recommended, whereas catchments of 100 ha require resolutions of 3 min and 2 km. The most common operational radar networks do not meet these requirements. Jordan, Seed and Austin (2000) evaluated the error that is introduced with the coarsening of rainfall radar observations. Results showed that when aggregating 100 m and 10 s radar rainfall observations to 1 km and 5 min a 40 % error was introduced. Furthermore, Schleiss (2016) developed a geostatistical framework for quantifying the temporal evolution and predictability of rainfall fields and found that the predictable scales for convective events are depending on the spatial scale on the order of 12.7 km at 1 h, 5 km at 15 min and 1.6 km at 5 min.

[1] RAINGAIN is a transnational project aimed at improving the prediction of pluvial floods in cities. Within this project innovative tools and practices based on the use of high-resolution radar in four pilot cities (Leuven, London, Paris and Rotterdam) are developed and tested.

Peleg *et al.* (2018) analyzed the effect of sub-pixel scale spatial variability of extreme rainfall on the Intensity-Duration-Frequency (IDF) curves, which is a measure of quantifying extreme rainfall in engineering practice. The study was conducted based on 23 years of rainfall radar data of 1 km and 5 min resolution and a very dense rain-gauge network in Northern Israel. The radar derived IDF curve represents a mean areal precipitation, neglecting the spatial variability within a pixel. Rain-gauge-based IDF curves were used to test the radar subpixel rainfall variability. Results showed that the mean areal radar rainfall underestimated most of the extreme rainfall rain-gauge values with an average of 70%. This variability increased with longer return periods.

1.2 Land-use resolutions

Concerning the runoff, there are different approaches to approximate the runoff coefficient. Many studies underlined the dependency of runoff coefficients on rainfall by calculating runoff coefficients for their study area through rainfall intensities, mean annual precipitation or return periods (Merz, Blöschl and Parajka, 2006; Young, McEnroe and Rome, 2009; Ahm *et al.*, 2013). Nevertheless, studies have shown that land-use changes have an impact on the runoff coefficient (Shi *et al.*, 2007; Sriwongsitanon and Taesombat, 2011). For this reason and also due to a matter of simplification, in practice standard runoff coefficients per land-use are often applied (Oregon Department of Transportation Highway Division, 2014; Storm Water Management Shiawassee County, 2015; Californian Environmental Protection Agency, 2016). This is used especially for the rational method where design discharges are calculated by multiplying runoff coefficient and rainfall intensity, assuming a steady state runoff.

When including land use characteristics to the water balance, the sensitivity towards the different available land use data resolutions becomes relevant (Rodriguez, Bocher and Chancibault, 2013).

Branger *et al.* (2013) assessed the influence of land use data on the water balance on a 150-km^2 large catchment close to Lyon (France). The authors found that five land use classes and land use data resolutions ranging from 2.5 m to 10 m in a distributed hydrological model, were sufficient to give quite accurate results. Nevertheless, the authors suggest that when looking at smaller catchments than the one presented in this study, higher spatial resolutions of the land use data might be of high relevance. Jacqueminet *et al.* (2013) found land use data resolutions of 0.5 m to 2.5 m useful to apply in distributed hydrological models at catchment scales ranging from a few square kilometers to 100 km^2.

1.3 Previous research on Rotterdam

Due to climate change and urbanization, the understanding of the hydrological response is becoming increasingly important. Delta cities such as Rotterdam (Netherlands) want to develop early flood warning systems and reduce floods as well as Combined Sewer Overflows (CSOs). According to the KNMI'06 scenarios, by 2100 hourly precipitation intensities in the Netherlands will increase between 13 and 81% and the extreme rainfall intensities between 25 and 108% (van Oldenborgh, van Meijgaard and Attema, 2011; Bessembinder, Wolters and van Hove, 2013). The resulting increase in storm water can put pressure on the urban drainage system and lead to an increase in floods and CSO polluting surface waters. Understanding the city's hydrological response to heavy rainfalls is a particular challenge in Rotterdam as it has a complex urban drainage system due to its small elevation differences, large storage facilities and its looped structure (cross-boundary conduits that make it difficult to exactly determine the way the water in the sewer flows) (Bruni et al., 2015). To improve this understanding, pumping volumes from the sewer districts and water levels measured at 21 CSO weirs since June 2016 can be used (Liefting & de Haarn, 2016 cited in Mulder, 2017). Besides, a new dual-polarimetric X-band radar was installed in the city Rotterdam itself in July 2017 in addition to the existing radar network used for the entire country. However, data from the X-band radar is not available yet.

On the basis of the available data sets related to floods in Rotterdam, several studies have been conducted. Bouwens (2017) studied the flood vulnerability of the city on the base of citizen flood complaints from 2012-2016 and found that the degree of imperviousness substantially influences the probability of flood occurrence. Based on the relation between heavy rainfall and citizen's flooding reports and CSO from 2010 - 2016, Bouwens *et al.* (2017) identified different thresholds after which the probability of flood occurrence increases significantly. For the rainfall intensities, the thresholds

are at 6 mm/15 min and 11 mm/hour and for the imperviousness at 70 % (±4 %). This study highlights the importance of scales, spatial variability and spatial aggregation of rainfall. It also shows that on a daily timescale, antecedent rainfall does not serve as a good predictor for urban pluvial flooding. However, smaller timescales could possibly give different results. (Bouwens *et al.*, 2017)
Mulder (2017) investigated the hydrological response time of the urban drainage system of Rotterdam comparing radar rainfall data and the sensor data at the CSO weirs (June 2016 – December 2016). Surprisingly, no significant relationship between the hydrological response time and the imperviousness or other rainfall characteristics such as rain event duration, intensity and cumulative volumes in the previous period was found. This was explained by the fact that spatial variability in rainfall and imperviousness was not taken into account, although it should be an important factor to consider. For this reason, the author suggests considering multiple CSO sensors per district. Further, it was concluded that the highly variable observed hydrological response times are mainly associated with the fact that only one peak per event was considered and with assumptions on the definition of the rain event. By choosing a short dry period between rain events, large outliers were created in the response times as previous events may have filled up the system leading to a quick response to the analyzed event. Additionally, results showed that the runoff coefficient is related to antecedent rainfall. This explains why the highest runoff coefficients were found in the wettest months (June and July).

In order to find optimum rainfall resolutions, Bruni *et al.* (2015) conducted a model-based study for Rotterdam analyzing the sensitivity of urban hydrodynamic response to high-resolution radar rainfall according to spatial rainfall characteristics and urban catchment properties in the city. The authors tested resolutions ranging from 1 to 10 min and from 100 to 2000 m. The model was built using SOBEK-Urban software (Deltares, 2014 cited in Bruni *et al.*, 2015), a semi-distributed model consisting of a lumped runoff-model incorporating evaporation, infiltration, surface storage and surface runoff, and a one-dimensional hydraulic model for pipe flow. Results showed that if the spatial resolution of the rainfall is lower than half of the catchment size, the rainfall volumes mean and standard deviations decrease due to the smoothing of rainfall gradients. For spatial resolutions similar to the size of the storm, the maximum computed water depths deviated from 10 to 30%. Moreover, the study found sensitivity to temporal resolution to be lower than to spatial resolution. Nevertheless, aggregating the original 1 min resolution to 5 and 10 min increased the rainfall correlation length up to 45% of the original de-correlation length. Additionally, the temporal aggregation led to peak time shifts of up to 6 min for all rainfall events. The authors concluded that critical thresholds depend on the relationship between rainfall resolution and model scales.

1.4 Objectives

These studies demonstrate that scales play an important role in the dependency of hydrological response to both, rainfall radar and land-use data. Therefore, this additional thesis aims at analyzing the effect of spatial rainfall radar and land-use resolutions on the water balance at event and district scale, based on field observations of radar rainfall, water levels at combined sewer overflow weirs, volumes of pumping stations as well as land-use maps on Rotterdam as case study.

In particular, this study will address the following research questions:

- How well does the water balance close?
- What is the influence of spatial radar rainfall resolution on the water balance?
- What is the influence of spatial resolution of land-use on the water balance?
- How do the resolutions of land-use and radar-rainfall interact in relation to the urban water balance?

This work is performed within the framework of project MUFFIN[2] (Multi-scale Urban Flood Forecasting) project, of which Rotterdam is part of and which tries to determine: “What spatial and

[2] The Muffin project involves different European universities and partners with the aim of developing innovative systems and solutions that diminish the adverse effects of urban flooding (*MUFFIN Project*, 2017).

temporal resolutions are necessary to adequately capture and predict rainfall patterns responsible for urban flooding?".

2. Catchment characteristics and available datasets

2.1 Characteristics of the Rotterdam catchment area and storm water drainage system

This study is conducted for Rotterdam, located in the West of the Netherlands in a flat, lowland polder area. It is a city of approximately 638 000 inhabitants (*Statline - Statistics Netherlands*, 2017) and covers an area of 319 km^2 (Hoyer *et al.*, 2011). Rotterdam has a temperate climate and predominantly westerly winds. The mean annual rainfall in Rotterdam is 846 mm, with little seasonal variation (Koninklijk Nederlands Meteorologisch Instituut, 2016).
The urban drainage system of Rotterdam is very complex for various reasons. As flow directions may change in lowland areas, blockages in the sewer system play a significant role. In order to increase the robustness of the network to blockages, the sewer system of Rotterdam is looped (Ten Veldhuis and Olsen, 2012). This makes it more difficult to distinguish flow paths during storm events (Berne et al., 2004 cited in Ten Veldhuis and Olsen, 2012), as they cannot be defined based on topography or network configuration (Bruni *et al.*, 2015).
Under the concept "retain, store, drain water" the city included several cost-effective multifunctional solutions such as the Water Square at the Benthemplein (Bouwens *et al.*, 2017) and an underground storage facility that is capable of holding 10 000 m^3 during heavy rainfalls (Bruni *et al.*, 2015). The water that exceeds the capacity of the system flows through the CSO weirs into open surface water or is transported via pumps into the river Meuse (overflow pumping) (Bruni *et al.*, 2015; Bouwens *et al.*, 2017). The latter is a control action with a higher preference over CSOs, that can only be executed in sewer districts situated along the Meuse to avoid CSOs or street flooding (Bouwens *et al.*, 2017).

2.2 Sewer district selection

Only certain districts in Rotterdam were selected for the analysis. This selection was based on the following criteria:

- The chosen districts are preferably independent of other sewer districts or do only receive small amounts of water from other sewer districts.
- A minimum of one CSO is monitored in the district (to reduce uncertainties in CSO overflows).
- The sewer system is well mapped and the storage volume of the sewer is known (or can be estimated).

This selection resulted in three sewer districts: Spangen (5), Lombardijen (30) and Ijsselmonde (36). The districts have an area ranging between 3 and 6 km^2 (see Table 1). These three sewer districts were also studied by Mulder, 2017. Spangen is a very small independent sewer district with only one CSO. The water levels of this CSO are monitored. This is highly interesting because it eliminates uncertainties related to overflow estimates of non-monitored CSOs. Lombardijen also has an independent sewer system with a much larger surface area and higher amounts of CSOs. It has 14 CSOs out of which two are monitored. Ijsselmonde is interesting because of its very large surface area. Another specialty of this district is, that it contains a pump, which can directly pump into the river Meuse when the system's capacity is reached (OB). Nevertheless, this district is not completely independent of other sewers. It receives water from district 29, which is a very small adjacent district. This district also contains an OB and three unmonitored CSOs. Lombardijen also has first results of the 3Di model developed for the city, which can be interesting for future research (Schuurmans and Leeuwen, 2017). Figure 1 shows an overview of the selected areas with the location of the different pumps and the monitored weirs.

Table 1: Properties of selected districts

District	Area [km2]	Amount of CSOs (monitored)
5	0.57	1 (1)
30	2.92	14 (2)
36	6.34	21 (3)
36 incl. 29	7.02	24 (3)

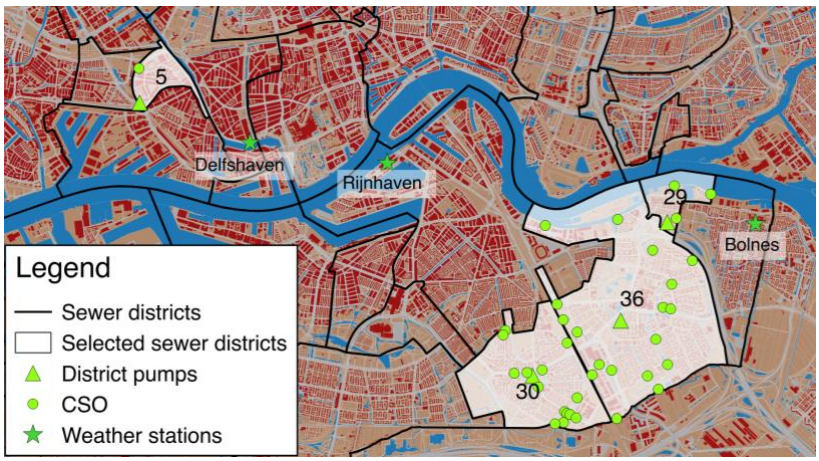

Figure 1: Study area

2.3 Maps

For the spatial analysis, three land use maps of Rotterdam of different scales of detail from the *Publieke Dienstverlening op de Kaart* (PDOK) portal were used (*PDOK - Publieke Dienstverlening op de Kaart*, 2017). The three land use maps with their corresponding scales are shown in Table 2. Worth to mention is that TOP50NL and TOP100NL are maps derived through coarsening from the original resolution TOP10NL map. All three maps contain four main land-use classes: "Gebouw" (*buildings*), "Waterdeel" (*water*), "Wegdeel" (*streets*), "Terrein any" (*other terrains*). All classes contain sub-categories. Here, the *other terrains* class contains very different land-uses such as *agricultural areas, grasslands, built areas*, and *train rails* whereas the other classes contain rather similar land-uses. In this analysis, only impervious areas are considered as explained in further detail in 3.1. These areas are represented by the classes or sub-categories *buildings*, *streets* and *built areas*. The effect of coarsening in the resolution of the used land-use maps on the percentage of impervious areas in the three districts is shown in Table 2. The TOP10NL map has a much higher level of detail and the impervious areas are composed by *buildings* and *streets*, whereas in the TOP100NL map the impervious areas are only composed by built areas, without differentiating between buildings or streets. The large loss in detail featured by the TOP100NL map leads to a difference in imperviousness of a factor 2 between the finest and the coarsest land-use map (see Table 2). These large differences are expected to have a strong impact on the results. The differences in rainfall resolution are going to be discussed in 3.4.

Table 2: Land use maps with corresponding scales and percentage of impervious areas

Map	**Scale**	**Percentage of impervious areas per district [%]**		
		5	**30**	**36**
TOP10NL	1:5.000 to 1:25.000	51.5	30.2	31.0
TOP50NL	1:50.000	60.3	40.1	38.6
TOP100NL	1:100.000	89.0	74.2	62.7

For the estimation of the sewer systems volume the *Rioolenplan* from the Rotterdam open data store portal was used (*Rotterdam open data store*, 2018). This gives information about the location, length, shape and diameter of the sewer pipes.

2.4 Datasets

Rainfall

Two different sets of rainfall were used for this study. Rainfall events were selected based on the data of the weather stations of the TU Delft (*Weather TU Delft*, 2018). The actual water balance analysis is based on radar rainfall data, which is considered more appropriate to capture spatial variability, compared to rain gauge data as outlined in Chapter 1. The data set includes 5 min radar data of 1 km x 1 km resolution provided by the KNMI. The data is corrected with KNMI weather stations to reduce underestimation of accumulated rain. Due to the availability of the CSO weir level data, the rainfall

from June 2016 to December 2017 was used. For the period from June 2016 to January 2017 the dataset is based on the composites of radar reflectivity from both KNMI weather radars (De Bilt at 52.103 degrees N, 5.179 degrees E and Den Helder at 52.955 degrees N, 4.79 degrees E). From January 2017 onwards the contribution of the radar in De Bilt was replaced by a new radar in Herwijnen (5.1381 degrees N, 51.8369 degrees E). (KNMI, 2017)

Evaporation
The evaporation used for this study was taken from the KNMI (KNMI, 2018). The dataset consists of interpolated, daily Makkink evaporation averages based on 7 to 35 automatic weather stations of the KNMI. This tiff file covers the Netherlands with a 1 km grid.

District pumps
Pumping data of the three district pumps, transporting the sewer districts' wastewater to the treatment plant was provided by the municipality of Rotterdam in time steps of 1 min. Additional to these, the pumping volumes of the large pump from district Ijsselmonde (36) discharging directly to the river Meuse were given at 1-min temporal resolution. The pumping volumes of the OB of district 29 and of the pump discharging from district 29 towards district 36 were not available for this study. All districts contain data gaps lasting for several hours. More information about the effect of these will be given in section 4.

Combined sewer overflow
The monitoring program of the water level at 21 CSO weirs over 13 districts was implemented in June 2016 (Mulder, 2017). The 1-min water level data was provided by the municipality. In addition to this, rough estimates of overflow volumes were provided for the monitored CSO weirs, which are probably based on a transfer function translating water levels measured at the overflow weirs into overflow volumes. Nevertheless, exact information on how these estimates were obtained or on how rough they are is not available.

3. Method

3.1 Water Balance

This study is based on a water balance analysis for the urban sewer network of Rotterdam. The system boundaries for this water balance are given by the sewer network within sewer district boundaries and the associated runoff areas. In the ideal case, the water balance would close as follows:

$$V_{In} - V_{Out} - \Delta S = 0 \qquad (Equation\ 1)$$

Where V_{in} is the volume entering the system, V_{out} the volume leaving the system and ΔS the change in storage within the system between the start and the end of the event. In this case the inflow is composed as follows:

$$V_{In} = V_P + V_{DWF} + V_{GWI} \qquad (Equation\ 2)$$

V_P represents the surface runoff volume, V_{DWF} the volume of the dry weather flow (DWF) and V_{GWI} the groundwater volume entering the system. The surface runoff is only composed of the rainfall measured over streets, roofs and parking areas. Rainfall on pervious surfaces (gardens, parks, green zones along roads) is assumed to infiltrate directly to groundwater. As groundwater it can then enter the system as V_{GWI}. The percentage of street, parking and roof areas for each district are shown in Table 3. These percentages are based on the information of the land-use map with the highest resolution (TOP10NL).

Table 3: Percentages of impervious land use types of the total area

District	Roofs [%]	Streets and Parking [%]	Sum of impervious area [%]
5	31.8	19.7	51.5
30	13.2	16.9	30.2
36	13.4	17.6	31.0

According to van der Linden (2012), Rotterdam faces groundwater and river water inflow to the sewer, especially in areas of the city where the pipes have not been replaced in the last years. In practice, this difference can be observed by a groundwater level rise of around 30 to 40 cm after old pipes are replaced by new ones. For an average pipe diameter of 500 mm the groundwater inflow to the sewer is at 0.3 l/s per km of pipe on a dry day (van der Linden, 2012). Leidraad Riolering determined the inflow to be between 0.1 – 1.1 l/km/s (Leidraad Rioleering, 2007 cited in van der Linden, 2012). On average, the GWI is in the same range as the DWF.
In order to obtain a local estimate of the DWF and the GWI for this analysis, the pumping volumes of the district pumps were used. The start of a rain event in this study is defined as the moment when it rains after a dry period of 12 hours (the complete definition will be given in 3.2). For this reason, the average hourly pumping rate during the four hours previous to the start of an event was calculated per district. These volumes represent a sum of DWF and GWI, as it is not raining during the four hours prior to an event. One would expect that during the night (3 a.m.) the pumped volumes would be lower than in the afternoon (6 p.m.) as the water consumption and thus, the DWF during the night is lower. This would mean that the pumped volume during the night would be mainly composed by the GWI. Nevertheless, this was not the case for the analyzed events. This could be caused, for instance, by rain prior to the 12 hours of dry period, that is still present in the sewer system and contributing to the pumped volumes. In order to reduce the influence of the uncertainties introduced here, the mean of hourly pumping rates (in the 4 hours prior to an event) of all events was taken per district. This resulted in district-specific hourly means composed by DWF and GWI. These hourly rates could then be multiplied with the corresponding event length to obtain the volume entering the system during one event. The municipality's report *Rioolvreemdwater* of the Waterschap Hollandse Delta (2013) contains district-specific annual averages for DWF and GWI in mm/d. This means that values were given per each sewer district in Rotterdam. The DWF is based on the number of inhabitants and companies but also on drinking water consumption. The GWI is based on the pumped volumes during dry periods, after subtracting the DWF. The proportion of DWF and GWI given per district in this report was used to split the previously obtained volumes into DWF and GWI.

The outflow is composed as shown in Equation 3, where V_{Pump} describes the pumped volumes, V_{CSO} the volumes flowing through the CSOs into open surface water, $V_{leakage}$ the volume leaving the system through leaking pipes and V_{Evap} the evaporated volumes.

$$V_{Out} = V_{Pump} + V_{CSO} + V_{leakage} + V_{Evap} \qquad (Equation\ 3)$$

V_{Pump} corresponds to the volumes pumped by the district sewer pumps and in the case of district 36 also the pump pumping into the river Meuse. V_{CSO} represents the volumes flowing through the CSOs from the sewer system into open surface water. This includes not only the volumes of the monitored CSO weirs but also the estimates of the non-monitored. These volumes were estimated, assuming that the water levels within the whole sewer district correspond to the average water level at the monitored weirs. Here, a large uncertainty is introduced because especially in larger sewer districts such as district 30 and 36 the water levels within the same sewer can vary. For the case of district 5, there is only one CSO weir, which eliminates this uncertainty. Water levels of the monitored CSOs were used to calculate all overflow volumes (monitored and non-monitored) applying equation 4. The weir levels and widths were given for all CSOs (including non-monitored) by the municipality. Here, b is the weir width in meters, H the height of the water level over the weir in m NAP and C_d the dimensionless discharge coefficient, which should be between 0.6 and 0.7 (Butler and Davies, 2004). For this analysis, the coefficient was set to 0.6. The gravity g was computed as 9.81 m/s^2. The calculated CSO volumes were on average 26% larger than the estimates provided by the municipality. It would be interesting to compare the two calculations. Nevertheless, there was no information available on how the volumes were estimated.

$$Q = C_d \frac{2}{3} b \sqrt{2g} H^{\frac{2}{3}} \qquad (Equation\ 4)$$

It should be noted that during heavy rainfall events the open surface water at the CSO and the sewers might become one system. If the suction of the pumps is very strong it even partly empties the surface

water. By comparing the surface water levels measured by the sensors outside of the weir to the weir height, the backflow occurrence could be detected. During the events analyzed within this study no backflow was occurring.
The pipes in Rotterdam are mainly located at 2.5 m below ground level whereas the groundwater level is between 0.8 – 1.4 m under ground level and the open water surface is at 1.2 m under ground level (van der Linden, 2018). Thus, only with few exceptions the sewers are submerged in groundwater. The areas that have been chosen for this study have submerged pipes. Under this condition, water losses from the pipes to the surrounding ($V_{leakage}$) can be neglected.
Although evaporation is often assumed to be zero during the moment it actually rains (Mansell and Rollet, 2008), in the dry periods between moments of rain (still within the defined event), evaporation can occur. The events in this study have lengths of more than a day and include longer dry periods during which evaporation can occur. For this research, daily gridded Makkink evaporation was used and applied to the time series of the corresponding events. More details about this are given in 3.4.

The change in storage is estimated by multiplying the change in water level between the start and the end of the event at the CSO weirs with an equivalent area. This area is calculated as follows. First, the total volume of the sewer is divided by the sum of the length of all pipes resulting in an average cross-section. Then, the square root of this cross-section is taken assuming a simplified quadratic cross-section. This results in an average height and width of the sewer. The equivalent area is calculated by calculating the average width with the sum of the length of all pipes.

Concluding equation 1 can also be written as follows:

$$V_P + V_{DWF} + V_{GWI} - V_{Pump} - V_{CSO} - V_{leakage} - V_{Evap} - \Delta S = 0 \qquad (Equation\ 5)$$

3.2 Definition of a rain event

In literature, several definitions of a rain event can be found. Commonly, a rainfall event is defined as a period, or sequence of periods, of continuous rainfall, separated by a dry period between the previous and the subsequent rainfall event (Brunetti et al. 2010; Peruccacci et al., 2012; Gariano et al., 2015a cited in Peruccacci et al., 2017). However, this maximum dry interval is defined depending on regions, seasons and can vary drastically, for example, 80 minutes or 96 hours (Mutzner, 1991; Peruccacci et al., 2017). This complicates the comparison of studies in this field. As this study is a follow up of previous research on Rotterdam, a rain event was defined on the basis of the work and recommendations of Mulder (2017). The start of a rain event is defined as the first moment when precipitation is measured after a certain dry period and the end as the moment when no precipitation was measured for two hours (Gaál, Molnar and Szolsgay (2014) cited in Mulder, 2017). From his research, he recommended using a longer duration of dry periods to separate rain events. This threshold was set to 12 hours for this study, which implies that the threshold for setting an end to a rain event is also a minimum of 12 hours without precipitation. This is the time it takes until the system empties. Another point to consider is that the longer the required dry period between events, the larger the influence of small, relatively continuous flows like DWF and groundwater infiltration is going to be. While Mulder (2017) used a minimum of 5 mm of accumulated rainfall, a minimum of 10 mm was used for the present study to focus on the largest events. The maximum length of an event was limited to 2 days.

3.3 Selection of rain events

The selection of the rain events was made on the basis of the three TU Delft weather stations *Bolnes*, *Rijnhaven* and *Delfshaven,* which were closest to the study area (see Figure 1). The definition of a rain event for this study resulted in 30 (Bolnes), 31 (Rijnhaven) and 36 (Delfshaven) events over the period from 01.06.2016 to 31.12.2017 with a rainfall volume larger than 10 mm (see Table 4).

Table 4: Events based on weather stations

Rainfall stations	Number of events larger than 10 mm
Bolnes	30
Rijnhaven	31
Delfshaven	36

These events larger than 10 mm were ranked according to total volume for each station. Seven events were part of the top ten of each of the stations. Four additional events were selected based on the largest volumes across the different stations. To transfer these events to the radar data, the earliest starting time and the latest ending time were chosen from the three weather stations.
All 11 selected events were in the warm season (June to October) and thus only reflect rain (no snow) and convective events. The length of each rainfall event is shown in Table 5. As described in 3.2, this is the time between the first moment when precipitation is measured after a 12-hour dry period and the moment when no precipitation was measured for 12 hours. This means that the 12 hours without rain at the end of the event are included in the event length. The rainfall duration within the total event length was on average 15.5% (see Table 5 for the event-specific rainfall duration). This relatively low percentage is given due to the definition of the rainfall event. The dry period of 12 hours between events leads to very long events with several dry periods within the event. Moreover, during the 12 hours at the end of the event it does not rain. The CSO occurrence differed per event and district. The analysis of the rainfall events that did not trigger a CSO eliminates the uncertainty associated with computing combined sewer overflow volume.

Table 5: Eleven selected events with their characteristics

Event	Event Length [h:min]	Rainfall duration within event [%]	Rainfall [mm]	CSO occurrence in districts
00	56:05	11.2	28.7	
01	49:05	19.3	27.3	36
02	37:25	6.8	42.9	5, 30, 36
03	38:10	17.0	26.5	36
04	31:10	13.0	25.0	
05	54:40	25.3	49.1	36
06	55:40	11.2	36.5	
07	55:55	9.2	33.3	5, 30, 36
08	46:05	18.6	30.3	
09	56:55	22.6	45.8	
10	58:45	16.0	30.6	36

3.4 Spatial resolutions

To set a range for the spatial rainfall radar resolutions analyzed in this study, a few references can be used. In the last decades, a widespread increase of radar rainfall estimates that are generally provided by national meteorological services at 1 km/5-10 min resolutions has taken place (Ochoa-Rodriguez et al., 2015). It makes sense to choose operational resolutions that are typically available. Most commonly, national radar networks operate at 1 km/5 min (e.g. Netherlands, UK, France) and others operate at 1 km/10 min (Malaysia) or 500 m/5 min (Belgium)(Ochoa-Rodriguez et al., 2015). The sewer district size of only around 5 km^2 limit the spatial scales that make sense to analyze. The model-based study on Rotterdam uses resolutions varying from 100 m/1 min to 3000 m/10 min (Ochoa-Rodriguez et al., 2015). For this reason, spatial resolutions varying from 1 to 3 km were chosen. As the results suggested that there could be an optimal rainfall resolution to close the water balance, which is larger than 3 km, the resolution 5 and 10 km were added (see 4.2). This results in radar pixel sizes ranging from 1 km^2 to 100 km^2, which is larger than each of the district areas (0.6 km^2, 2.9 km^2 and 7.0 km^2). Due to the specific location of the sewer districts within a radar cell the rainfall starts to be homogeneous from a rainfall resolution of 5 km for district 5 and of 10 km for districts 30 and 36.
To simulate different resolutions in land-use, different datasets from the PDOK were used (TOP10NL, TOP50NL and TOP100NL). These maps do not have specific resolutions but are recommended for different scales as mentioned before. The different spatial resolutions of rainfall radar and land-use will be tested and compared to each other. Five different spatial rainfall radar resolutions and three different land-use resolutions will be combined in a matrix resulting in 15 different cases as shown in Table 6. The highest resolution (A1) will be used as a reference. Generally speaking, coarser resolutions in space lead to more uniform inputs, both for rainfall and land-use. Thus, they give a larger bias but also reduce noise (contamination, clutter). This also opens the possibility of giving better results. In particular, it could be that the radar cell is shifted in space or time and thus, the

location or timing of the high rainfall intensity is wrong. For higher resolutions the sensitivity to these shifts increases whereas in coarser resolutions it decreases.

Table 6: Combinations of rainfall radar and land use resolutions

	1 km	2 km	3 km	5 km	10 km
TOP10NL	A1	A2	A3	A5	A10
TOP50NL	B1	B2	B3	B5	B10
TOP100NL	C1	C2	C3	C5	C10

For each event, the corresponding radar files were summed up to a single file, which were then read into QGIS. In this way, the rain over the impervious areas, which is the volume assumed to go into the sewer system, could be calculated. These summed rainfall files were aggregated to the coarser resolutions of 2 km, 3 km, 5 km and 10 km by taking the average or the corresponding cells of the highest resolution. Then for each event, the different rainfall and land-use resolutions were combined. As shown previously in Table 2, the coarsening in land-use resolution leads to input changes of a factor of 2. Table 7 includes the mean rainfall volumes for each district and each resolution combination. The individual rainfall volumes per event are shown in the Appendix (see 7.1). It becomes visible that changes in rainfall radar resolution cause much smaller changes in rainfall input than changes in land-use resolution. For some cases the rainfall increases and for other it decreases with a coarsening in rainfall resolution. This is expected to influence the results as well.

Table 7: District-specific rainfall input (means of all events) [m^3]

District	5	30	36 (incl. 29)
A1	10899	27816	68426
A2	10591	26625	65742
A3	11184	26447	65265
A5	10259	27193	57915
A10	10009	31342	78547
B1	12822	36992	79339
B2	12469	35316	75923
B3	13161	35180	75813
B5	12070	36355	67411
B10	11775	41691	92405
C1	18922	68550	131789
C2	18370	65538	122148
C3	19413	65260	121549
C5	17813	67586	108519
C10	17378	77486	149391

A similar procedure to the rainfall calculation was applied to obtain the evaporation volumes. The evaporation was given in a tiff file as interpolated gridded daily values. Although the grid consists of pixels of 1 km, adjacent pixels have hardly any variation, as it is interpolated data between weather stations. For this reason, for each district the evaporation estimates at the highest resolution of 1 km were applied to the three different land-use maps (three different impervious areas per district) for the corresponding time series, resulting in three different evaporation volumes per event (and per sewer district). On average this resulted in an evaporation rate of 2 mm per day, which is within the regular range of assumed values of 0-5 mm/d (van der Linden, 2018).

4. Results and Discussion

The 15 different combinations of rainfall radar and land-use resolution for the three sewer districts and eleven events resulted in 495 water balances, which, if the estimates are correct, should be zero.

4.1 Highest resolution

In order to obtain a first understanding of the composition of the different components of the water balance, all events were plotted as bar charts in the highest resolution (A1). Figure 2 shows the most representative events and outcomes. In the figure, each row of graphs represents one event and each column of graphs a sewer district. In most of the cases, the water balance is larger than zero, as shown in Event 0 and Event 4 in Figure 2, meaning that more water enters than leaves the system. This could

either mean that the input components such as the rain but also the DWF and the GWI are overestimated, that evaporation is underestimated, that pumping data is faulty or a combination of several of these aspects.

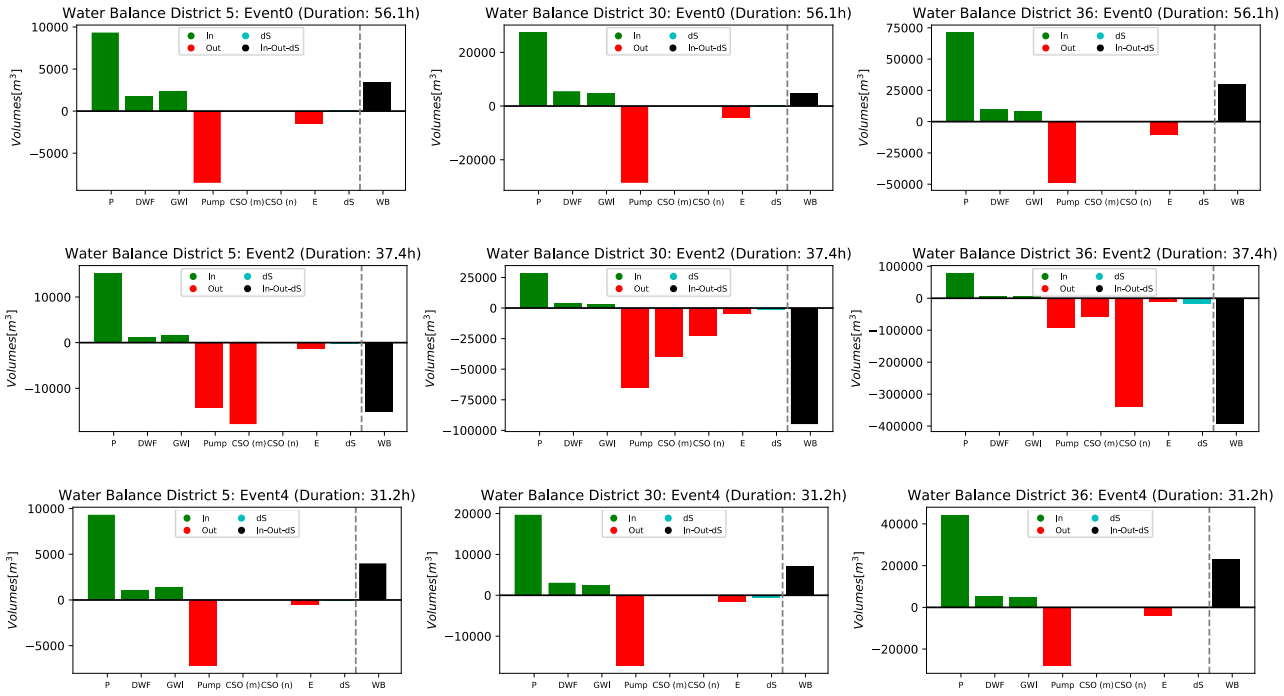

Figure 2: Highest resolution (A1) water balance compositions of selected events

Comparison of rainfall radar data to rain gauges

The variety of errors that radar data features described by Schellart, Shepherd and Saul (2012) can contribute to the imbalance. To test if the radar rainfall totals are overestimated, they were compared to the weather stations on the ground. Figure 3 shows the event-specific mean rainfall volumes from the weather stations and the radar rainfall from all districts or weather stations. In Appendix 7.1 the comparison is made in more detail, where each bar represents the rainfall at one weather station or in one sewer district[3]. The comparison of the radar rainfall data and the weather stations shows, that there is no clear over- or underestimation of one of the two sources of data.

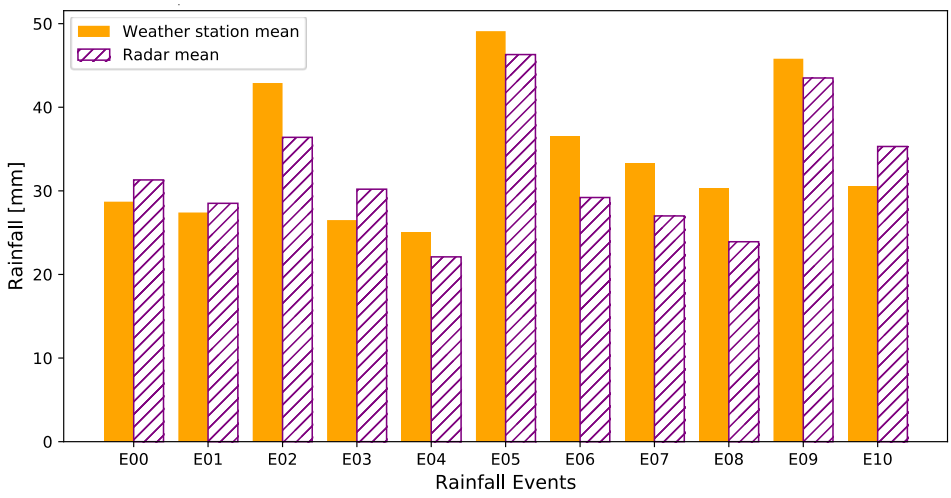

Figure 3: Comparison of mean rainfall volumes from the weather stations and the radar per event

[3] The bars per event are ordered in their geographical location from northwest to southeast in order to relate the sewer districts' radar volumes to the weather station. For some events some weather stations do not have a rainfall volume. This is most likely because the definition of the rainfall event did not register the rain occurring during this period as an event.

These differences between the two datasets could be explained by spatial heterogeneity of rainfall. Another possible explanation is that the accuracy of high-resolution rainfall estimates diminishes for higher precipitation intensities (Van de Beek et al., 2010; Leijnse et al., 2010 cited in Ten Veldhuis and Olsen, 2012). The events used for this research were selected according to the highest volumes within the time series. That does not immediately mean that they have the highest intensities but there is a high probability that this is the case, especially when considering that the proportion of the time where it actually rains during the chosen rain events is on average 15% only (see Table 5). As mentioned by Ochoa-Rodriguez *et al.* (2015), the drainage area size has an influence on the required resolution to properly represent the hydrodynamics. Thus, it could also be that higher resolutions than 1 km x 1 km are needed in this case to properly represent the spatially heterogenic rainfall because the sewer districts, especially Spangen (5), are quite small (0.6 km^2).
Although the radar rainfall does not seem to be overestimated it is still probable that the component V_P (runoff) is. The rainfall falling on streets, roofs and parking areas is fully going into the sewer, except for the evaporation. Infiltration was neglected here as the areas were assumed to be impervious. Nevertheless, the land-use classification does not give insight into the material of the different land-use classes but rather into its use. In the case of streets, for example, a sub-classification differentiates primary and secondary roads. It is possible that some of the areas classified as streets, roofs or parking areas are actually capable to infiltrate a part of the rain. This could be simulated by assigning runoff coefficients to the different land-use classes. These runoff coefficients would reduce the volumes. In this case, the evaporation component would be considered through this coefficient as well.

Dry weather flow and ground water inflow
As shown in Table 5, the duration of rainfall during an event is on average 15%. This means that the possible influence of uncertainty associated with DWF and GWI is relatively high. Figure 2 shows that Event 0 is approximately a day shorter than Event 4 although the total volume is comparable. In the longer event the DWF and the GWI contribute more to the water balance. This is because DWF and GWI are assumed to be constant over time, and during longer events a higher proportion of these components contribute to the water balance.
The DWF estimate could be improved by using actual data of the drinking water providers. Furthermore, the GWI was set to be a constant value. Nevertheless, the GWI reduces with increasing rainfall intensities. Therefore, it could be that the GWI is smaller than during the four hours prior to an event, which were used here to estimate the DWF and the GWI.

Pumping data gaps
Four of the eleven events contain gaps in the pumping data. Event 9 contains the largest gaps, with 80% of the time series missing. For this reason, it was excluded from further analysis. The remaining three events (6, 7 and 8) have data gaps ranging between 12 and 22%. However, the water balances do not differ much from the others without the gaps. This is a strong indication that the error on available pumping values is large.

CSO occurrence
The only water balances that are negative are the ones that include a CSO. This negative water balance closes even less than for the positive results (see Event 2 in Figure 2). This is an indication for an overestimation of the CSO volumes, although the weir coefficient C_d (see Equation 4) is already at its lowest value that is recommended in the literature (0.6) (Butler and Davies, 2004). The calculated CSO volumes in this study were on average 25% larger than the estimates from the municipality. Nevertheless, the calculation method and the data used to compute the volumes are not available. For this reason, it is difficult to assess the reliability of these volumes. There is a large uncertainty associated with the parameters used in this analysis such as weir height and width because varying values could be found in different sources.
Although the CSO and the OB pump of district 29 (which discharges into 36) was not taken into account, this effect is especially prominent for district 36. Sewer district 36 is the largest district with the highest amount of unmonitored CSOs and thus, also with the highest uncertainty considering water levels at all points within the district. Interestingly, when comparing the CSO volumes of district 30 and 36, the monitored CSOs (CSO (m)) contribute with a larger volume to the water balance than the non-monitored (CSO (n)). This is the opposite case for district 36. A possible reason for this is that

in district 36 several of the non-monitored CSO weirs are at similar heights as the monitored ones, so overflows can occur more easily, whereas the non-monitored weir levels in district 30 are much higher. Another important factor is the sewer district size. The calculation of the non-monitored CSO volumes is based on the assumption that the water level in the entire sewer district corresponds to the mean of the measured water levels at the monitored CSOs. The larger the sewer system, the higher is the probability that this assumption is incorrect.

Change in storage

The change in storage is the smallest component in the water balance. The only district where it becomes visible is district 36. This can be explained by its size: a larger area and sewer system takes more time to be emptied after an event. Therefore, it probably takes longer than the 12 hours set for this event definition.

4.2 Comparison of resolution combinations

To analyze the effect of the different resolution combinations across events of different rainfall intensities, the water balances were normalized by dividing the water balances by their specific rainfall (see Appendix 7.1). With coarsening land-use resolution, a general trend towards 1 can be observed. In contrast, the trend of coarsening in rainfall radar resolution is less clear, since it varies across events and districts. The events including a CSO occurrence have a negative water balance, whereas all the other events feature a positive water balance. The events with the pumping data gaps do not seem to vary significantly from the others.

A visual inspection of the histogram of the data showed a symmetric distribution. For this reason, the mean and the standard deviation were taken as a summary of the data (see Figure 4 and Table 8). In Appendix also the boxplots are shown (see 7.3). In Figure 4, the colors indicate equal rainfall radar resolution and the shapes indicate equal land-use maps. Based on the results in 4.1, the resolution-specific mean was first taken for all samples and then taken for the events and districts where no CSO occurred. This means that for Event 1, for example, only the water balances of district 36 were excluded, as the same event did not lead to a CSO in the two other districts.

CSO occurrence

In consistency with the results of the highest resolution (see 4.1) and the normalized water balances (see Appendix 7.1), the water balance is positive unless the event led to a CSO (see Figure 4). The effect that causes a positive water balance overlaps with the overestimation of the CSO volumes causing negative water balances. Thus, it becomes more difficult to identify and explain trends. As shown in 4.1, the CSO volumes are overestimated which is related to the high uncertainty, especially in the non-monitored weirs. To eliminate this uncertainty associated with computing combined sewer overflow volumes, the means of the events without a CSO were taken for the different resolution combinations.

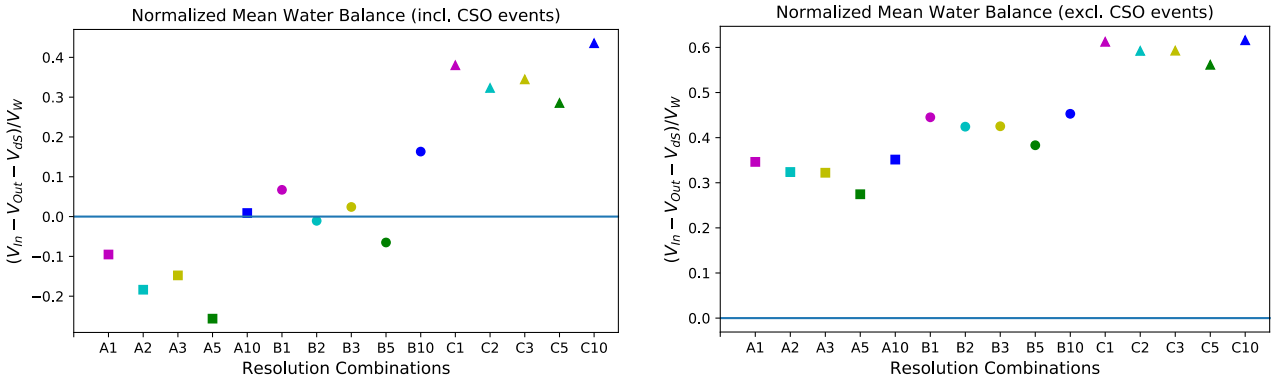

Figure 4: Normalized mean water balances incl. and excl. CSO events

Table 8: Mean and standard deviation of normalized water balances (excl. CSO)

	A1	A2	A3	A5	A10	B1	B2	B3	B5	B10	C1	C2	C3	C5	C10
Mean	0.35	0.32	0.32	0.27	0.35	0.45	0.42	0.43	0.38	0.45	0.61	0.59	0.59	0.56	0.62
Std.	0.15	0.17	0.16	0.17	0.19	0.11	0.12	0.12	0.14	0.14	0.06	0.08	0.07	0.10	0.08

Behavior with coarsening resolutions

When excluding the events that lead to a CSO, a clearer pattern becomes visible. In terms of land-use, the water balance tends to close less when land-use resolution becomes coarser (from A to C). This trend was to be expected, as the imperviousness of the sewer districts with the TOP100NL map is twice as high as with the TOP10NL map (see Table 2). This means that there is more area over which rain is taken into consideration and the possible overestimation of V_P has a larger impact on the water balance. These outcomes suggest that detailed land-use maps are of high importance to properly close the water balance.

In terms of rainfall, the water balance tends to close better by coarsening rainfall-radar resolution up to 5 km. At a rainfall resolution of 10 km the water balances closes less again. These results suggest that for each land-use resolution, there is an optimum radar rainfall resolution that minimizes the error on the water balance. This optimum seems to be at around a rainfall resolution of 5 km. As mentioned in 3.4, the coarser resolutions in space lead to more uniform inputs. Therefore, they have a larger bias but also reduce the noise as well as the sensitivity to measurement shifts in location or timing of high rainfall intensities. For this reason, the accuracy of high-resolution rainfall estimates diminishes for higher precipitation intensities Van de Beek et al. (2010), Leijnse et al. (2010) cited in Ten Veldhuis and Olsen (2012). In this case, it could be that this inaccuracy is smoothed out in the coarser resolutions and thus, presents better results. At 10 km the bias produced by having more uniform rainfall input seems to be larger than the reduction in noise and sensitivity to shifts and thus, the water balance closes less.

Table 8 shows that the standard deviation declines by coarsening land-use resolution, whereas it remains nearly constant over all rainfall resolutions within the same land-use. This indicates that the results for coarser land-use resolutions are more reliable. The mean of all samples (excl. CSO events) resulted in 0.45, which shows that the water balance does not close satisfactory.

Interesting to observe is the variation of the resolution-specific mean across the three different sewer districts (see Figure 5). In general, the water balance closes slightly more in district 30 and slightly less in district 36. As district 30 has the lowest imperviousness in the TOP10NL map the influence of overestimations of V_P are reduced. Further, it could be that the missing OB pumping data of district 29 contributes to a larger error in 36.

For all three districts the water balance closes less with coarser land-use resolution. This change is the strongest in district 30 and the least strong in district 5, which could already be seen from the changes in imperviousness throughout the different resolutions (see Table 2). The reason for this larger change in imperviousness is the way the different land-uses are distributed. In district 30 there are several small green areas in between pervious areas that in coarser land-use maps are taken as built areas, whereas in district 36, for example, the green areas are more concentrated in certain locations such that they are still considered as green areas in coarser land-use maps.

The outcomes concerning changes in rainfall radar resolutions differ more between the districts. In district 5, the changes are the least marked. This might be caused by its small size. The rainfall starts to be homogeneous from a resolution of 5 km onwards. For districts 30 and 36 the rainfall is only homogeneous in the coarsest resolution of 10 km. This could be the reason for the water balance closing less at 10 km. Nevertheless, it is rather surprising that in district 36 the optimum resolution is so prominent. Possibly, the other two districts have a similar peak but at a resolution that was not tested here, as for example 8 km.

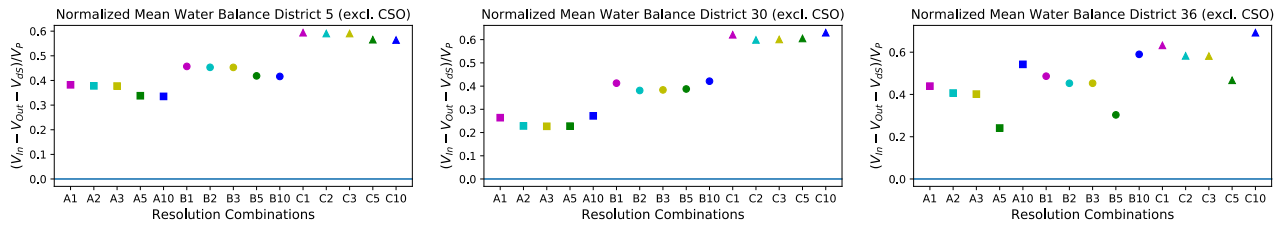

Figure 5: Normalized mean water balances per district excl. CSO events

Interaction of rainfall radar resolution and land-use resolution

In this section the research question about the interaction of the resolutions of land-use and radar-rainfall in relation to the urban water balance is going to be addressed. To evaluate whether the differences in rainfall radar resolution and land-use data have an influence on each other, the difference between the corresponding reference resolution and the coarser resolution was calculated in percentage per dimension (see Table 9 to Table 14).

In Table 9, Table 10 and Table 11, for each district the 1 km rainfall radar resolution of each land-use map was taken as a reference for the other resolutions (marked in blue). For example, the 2 km rainfall resolution with the TOP50 land-use map was calculated with reference to the 1 km-TOP50 combination. These three tables give insight into the influence of land-use resolution on changes in rainfall resolution. Comparing the different percentages within the same column, these three tables show that the percentage change for rainfall resolutions is smaller for the coarser land-use resolution maps.

In Table 12, Table 13 and Table 14 the TOP10NL land-use map is taken as a reference (marked in blue) meaning that these three tables give insight into the influence of rainfall resolution on changes in land-use resolution. Comparing the different percentages within the same row, there is a slight increase in change with coarser land-use resolution for district 5. The same is valid for districts 30 and 36 with some exceptions for the rainfall resolution of 10 km.

These tables suggest that there may be a relationship between resolutions in land-use and rainfall data. Nevertheless, more samples are needed to make strong conclusions on this question.

Table 9: Decrease in mean normalized water balances with rainfall resolution coarsening 5

	1 km	2 km	3 km	5 km	10 km
TOP10NL	100%	-1.1%	-1.3%	-11.6%	-12.3%
TOP50NL	100%	-0.8%	-0.9%	-8.4%	-8.9%
TOP100NL	100%	-0.5%	-0.6%	-4.8%	-5.0%

Table 10: Decrease in mean normalized water balances with rainfall resolution coarsening 30

	1 km	2 km	3 km	5 km	10 km
TOP10NL	100%	-13.4%	-14.0%	-13.8%	+3.0%
TOP50NL	100%	-7.6%	-7.0%	-6.1%	+2.0%
TOP100NL	100%	-3.6%	-3.3%	-2.6%	+1.4%

Table 11: Decrease in mean normalized water balances with rainfall resolution coarsening 36

	1 km	2 km	3 km	5 km	10 km
TOP10NL	100%	-7.4%	-8.6%	-45.1%	+23.5%
TOP50NL	100%	-6.9%	-6.9%	-37.6%	+21.3%
TOP100NL	100%	-7.9%	-8.0%	-26.1%	+9.4%

Table 12: Increase in mean normalized water balances with land-use resolution coarsening 5

	1 km	2 km	3 km	5 km	10 km
TOP10NL	100%	100%	100%	100%	100%
TOP50NL	+19.6%	+19.9%	+20.0%	+23.8%	+24.1%
TOP100NL	+55.3%	+56.3%	+56.4%	+67.2%	+68.2%

Table 13: Increase in mean normalized water balances with land-use resolution coarsening 30

	1 km	2 km	3 km	5 km	10 km
TOP10NL	100%	100%	100%	100%	100%
TOP50NL	+56.4%	+66.8%	+69.1%	+70.4%	+54.9%
TOP100NL	+153.3%	+162.0%	+164.8%	+166.0%	+131.6%

Table 14: Increase in mean normalized water balances with land-use resolution coarsening 36

	1 km	2 km	3 km	5 km	10 km
TOP10NL	100%	100%	100%	100%	100%
TOP50NL	+10.7%	+11.4%	+12.8%	+25.8%	+8.7%
TOP100NL	+43.9%	+43.2%	+44.8%	+93.7%	+27.6%

Evaporation

As a visual inspection of the water balance composition in Figure 2 already suggests, the evaporation does not have a very large influence on the outcome. Nevertheless, the results of the gridded daily evaporation data were compared to the case of zero evaporation to quantify the effect of the chosen evaporation data set. The normalized mean of the zero evaporation case of all districts, resolutions and events (excl. CSOs) was 0.56 compared to 0.45 of the previous results. Nevertheless, the mean variation across the different resolution combinations remains equal: showing worse results for coarsening in land-use resolution and slightly better results for coarsening in rain radar resolution. This indicates that more precise evaporation data could help closing the water balance, but the influence of resolution would not change much.

4.3 Recommendations

In order to evaluate the value of the conclusions it should be taken into account that there are several sources of uncertainty within this analysis. These uncertainties include the timing and location of the rainfall radar data, the influence of infiltration (which was neglected for this study), estimates on DWF and GWF, the errors and gaps of the pumping data as well as the interpolated evaporation data. In order to identify which dimensions have the strongest variations, a principle component analysis (PCA) would be useful for future studies. Here, only a qualitative evaluation of the sources of uncertainties is presented here to suggest which improvements should be prioritized.

In the first place, the water balance generally does not close properly showing that more volume enters than leaves the system. This is an important point to start with in order to increase the reliability of the results of the influence of changes in resolution. The largest components in the water balance are the rainfall input and the pumping data. Consequently, these two components should be prioritized for improvements in future research.

Probably, neglecting the infiltration within this water balance is one of the most crucial elements contributing to the error in this study. This could be improved by assigning runoff coefficients to the different land-use classes. By doing so the evaporation would not be considered separately anymore.

As the rainfall intensities of the radar data were comparable to the ones of the rain gauges, the radar data does not seem to generally overestimate the rainfall. Nevertheless, there could still be a shift in timing or location of the radar data. For this reason, it would be useful to compare the present rainfall data to other rainfall data such as the radar data from the *Lizard* of the municipality. It could be that more accurate rainfall inputs would change the effect that current coarsening in rainfall radar resolution has on the water balance.

The strong differences in behavior of the mean normalized water balances between the different sewer districts were rather unexpected. It would be interesting to test resolutions in between the analyzed ones, such as 4 km, 6 km, 7 km, 8 km and 9 km. This would show if districts 5 and 30 also have a rainfall resolution at which the water balances closes much more than at the other resolutions, as it is the case for district 36.

Furthermore, the reliability of the pumping data provided by the municipality is uncertain. It contains large data gaps of several hours for all pumps at the same time. This indicates that there was rather an error when pre-processing the data than a temporary failure of the pump or of the pumping record. Especially, considering the fact that the events containing data gaps did not differ a lot from the other events decreases the reliability of the entire dataset.

The most interesting events, especially for the municipality, are the extreme rainfall events that lead to CSOs. For this reason, it is important to be able to approximate the overflow volumes more accurately. As a first step, it would be interesting to compare the present calculation with the one of the municipality in terms of used formulas and input data. The reliability of the parameters such as the weir height and width is low, as different sources indicated different values. This has a large impact on the calculations. Another uncertainty is the estimation of the discharged volumes via the non-monitored CSO weirs. A denser observation network would be useful to be able to make more accurate estimations on discharge volumes and also on the change in storage.

The uncertainties associated with DWF and GWI estimates could be improved by using actual data of the water providing company in Rotterdam corresponding to the timing of the events.

A difficulty of this research was that, apart from the two dimensions of spatial scales, there are several factors varying across results such as different district sizes, CSO occurrences in some events and

different event lengths. This variety of dimensions complicates the assignment of trends to a specific variable. For future studies, it would be recommended to have more samples without variations, for instance, one district with many events of similar lengths.

5. Conclusion

The aim of this paper was to analyze the influence of spatial coarsening resolution in rainfall radar data as well as in land use data on the water balance. For this purpose, three different sewer districts in Rotterdam were analyzed. The results showed that, through all resolutions, the water balance does not close properly, as more volume enters than leaves the system. This is most probably related to the fact that the runoff areas went directly into the sewer system only considering evaporation. Infiltration on the runoff areas was completely neglected. By having a more detailed distinction between the different impervious areas this effect could be reduced. Also, the higher inaccuracy of radar signals for high-precipitation intensities could be responsible. Furthermore, the reliability of pumping data is uncertain, since the events that included long data gaps did not give significantly different results than the events without gaps. Events that led to a CSO clearly show that the CSO volumes are overestimated. This error multiplies with an increase in sewer district size, a higher amount of unmonitored CSOs and lower weir levels. Regarding the influence of rainfall radar resolution and land-use data, the main conclusions drawn from this research are that the water balance degrades remarkably with coarser land-use data detail and improves slightly with higher rainfall radar resolution until reaching a certain threshold where the error is minimized. After this threshold the water balance closes less. It must be noted that this is valid for the analyzed degrees of details in land-use and rainfall radar resolutions. It could be that the radar-rainfall resolution steps are smaller compared to the land-use resolution steps. A possible explanation for the better results with coarser rainfall resolutions is that at coarser scales, the noise as well as the sensitivity towards shifts in timing and location of the radar data is reduced. The changes with varying resolution combinations appear to be different in the three districts. Nevertheless, more resolutions in between the analyzed ones need to be tested in order to see if they actually differ. Finally, the results suggest that there might be a relationship between the variations in land-use resolution and the ones in rainfall radar resolution.

6. References

Ahm, M. *et al.* (2013) 'Estimating subcatchment runoff coefficients using weather radar and a downstream runoff sensor', *Water Science and Technology*, 68(6), pp. 1293–1299. doi: 10.2166/wst.2013.371.

Bárdossy, a. and Das, T. (2006) 'Influence of rainfall observation network on model calibration and application', *Hydrology and Earth System Sciences Discussions*, 3(6), pp. 3691–3726. doi: 10.5194/hessd-3-3691-2006.

Bell, V. A. and Moore, R. J. (2000) 'The sensitivity of catchment runoff models to rainfall data at different spatial scales', *Hydrology and Earth System Sciences*, pp. 653–667. doi: 10.5194/hess-4-653-2000.

Berne, A. *et al.* (2004) 'Temporal and spatial resolution of rainfall measurements required for urban hydrology', *Journal of Hydrology*, 299(3–4), pp. 166–179. doi: 10.1016/j.jhydrol.2004.08.002.

Bessembinder, J., Wolters, D. and van Hove, L. W. A. (2013) *Regiospecifieke klimaatinformatie voor Haaglanden en Regio Rotterdam*.

Bouwens, C. (2017) *Flooding observations in Rotterdam : mapping of flood - prone locations , flood vulnerability and risk analysis*.

Bouwens, C. *et al.* (2017) 'The relation between heavy rainfall and urban pluvial flooding : A case study for Rotterdam', (2015), pp. 1–19.

Branger, F. *et al.* (2013) 'Assessment of the influence of land use data on the water balance components of a peri-urban catchment using a distributed modelling approach', *Journal of Hydrology*. Elsevier B.V., 505, pp. 312–325. doi: 10.1016/j.jhydrol.2013.09.055.

Bruni, G. *et al.* (2015) 'On the sensitivity of urban hydrodynamic modelling to rainfall spatial and temporal resolution', *Hydrology and Earth System Sciences*, 19(2), pp. 691–709. doi: 10.5194/hess-19-691-2015.

Butler, D. and Davies, J. W. (2004) *Urban Drainage*. 2nd edn.

Californian Environmental Protection Agency (2016) *Runoff Coefficient (C) Fact Sheet*, *The Clean Water Team Guidance Compendium for Watershed Monitoring and Assessment State Water Resources Control Board*. Available at: http://www.waterboards.ca.gov/water_issues/programs/swamp/docs/cwt/guidance/513.pdf.

Einfalt, T. *et al.* (2004) 'Towards a roadmap for use of radar rainfall data in urban drainage', *Journal of Hydrology*, 299(3–4), pp. 186–202. doi: 10.1016/j.jhydrol.2004.08.004.

Fabry, F. *et al.* (1994) 'High resolution rainfall measurements by radar for very small basins: the sampling problem reexamined', *Journal of Hydrology*, 161(1–4), pp. 415–428. doi: 10.1016/0022-1694(94)90138-4.

Hoyer, J. *et al.* (2011) *Sustainable Water Management in the City of the Future Water Sensitive Urban Design Principles and Inspiration for Sustainable Stormwater Management in the City of the Future - Manual – Water Sensitive Urban Design*. Hamburg: jovis jovis Verlag GmbH.

Jacqueminet, C. *et al.* (2013) 'Land cover mapping using aerial and VHR satellite images for distributed hydrological modelling of periurban catchments: Application to the Yzeron catchment (Lyon, France)', *Journal of Hydrology*, 485, pp. 68–83. doi: 10.1016/j.jhydrol.2013.01.028.

Jordan, P., Seed, A. and Austin, G. (2000) 'Sampling errors in radar estimates of rainfall', *J. Geophys. Res.*, 105(D2), pp. 2247–2257. doi: 10.1029/1999jd900130.

Kavetski, D., Kuczera, G. and Franks, S. W. (2006) 'Bayesian analysis of input uncertainty in hydrological modeling: 2. Application', *Water Resources Research*, 42(3), pp. 1–10. doi: 10.1029/2005WR004376.

KNMI (2017) *KNMI Data Centre - precipitation - 5-min precipitation accumulations from climatological gauge-adjusted radar dataset for The Netherlands (1 km)*. Available at: https://data.knmi.nl/datasets/rad_nl25_rac_mfbs_5min/2.0 (Accessed: 6 January 2018).

KNMI (2018) *Evaporatin - gridded daily Makkink evaporation for the Netherlands*. Available at: https://data.knmi.nl/datasets/EV24/2?bbox=51.98,4.61,51.76,4.08&dtend=2017-12-31T22:59Z&dtstart=2016-05-31T22:00Z&q=evaporation (Accessed: 10 February 2018).

Koninklijk Nederlands Meteorologisch Instituut (2016) 'Jaaroverzicht neerslag en verdamping in Nederland (JONV)'. Available at: http://www.knmi.nl/nederland-nu/klimatologie-overzichten.

van der Linden, L. (2012) *Vreemd water, gezond verstand*. Hogeschool Rotterdam.

van der Linden, L. (2018) 'Interview on the 09.01.2018'. Rotterdam.

Mansell, M. and Rollet, F. (2008) 'The Effect of Surface Texture on Evaporation , Infiltration and Storage Properties of Paved Surfaces', pp. 1–10.

Mcmillan, H. *et al.* (2010) 'Input Uncertainty in Hydrological Models : An Evaluation of Error Models for Rainfall', *Journal of Hydrology*, 400(1–2), pp. 83–94.

Merz, R., Blöschl, G. and Parajka, J. (2006) 'Spatio-temporal variability of event runoff coefficients', *Journal of Hydrology*, 331(3–4), pp. 591–604. doi: 10.1016/j.jhydrol.2006.06.008.

Moulin, L., Gaume, E. and Obled, C. (2008) 'Uncertainties on mean areal precipitation: assessment and impact on streamflow simulations', *Hydrology and Earth System Sciences Discussions*, 5(4), pp. 2067–2110. doi: 10.5194/hessd-5-2067-2008.

MUFFIN Project (2017). Available at: http://www.muffin-project.eu/rotterdam-nl/ (Accessed: 10 December 2017).

Mulder, M. G. J. (2017) 'Additional Thesis The effect of the imperviousness on the hydrological response time of sewer districts Rotterdam', (January).

Mutzner, H. (1991) 'The significance of areal rainfall distribution for flows from a very small urban drainage catchment', *Atmospheric Research*, 27(1–3), pp. 99–107. doi: 10.1016/0169-8095(91)90011-K.

Ochoa-Rodriguez, S. *et al.* (2015) 'Impact of spatial and temporal resolution of rainfall inputs on urban hydrodynamic modelling outputs: A multi-catchment investigation', *Journal of Hydrology*. Elsevier B.V., 531, pp. 389–407. doi: 10.1016/j.jhydrol.2015.05.035.

van Oldenborgh, L. G. G. J., van Meijgaard, E. and Attema, J. (2011) *KNMI*. Available at:

https://www.knmi.nl/kennis-en-datacentrum/achtergrond/intensiteit-van-extreme-neerslag-in-een-veranderend-klimaat (Accessed: 8 December 2017).

Oregon Department of Transportation Highway Division (2014) *ODOT Hydraulics Manual - Appendix F - Rational Method*.

PDOK - Publieke Dienstverlening op de Kaart (2017). Available at: https://www.pdok.nl/nl/producten/pdok-downloads/basis-registratie-topografie/topnl/topnl-actueel (Accessed: 15 January 2018).

Peleg, N. *et al.* (2018) 'Spatial variability of extreme rainfall at radar subpixel scale', *Journal of Hydrology*. Elsevier B.V., 556, pp. 922–933. doi: 10.1016/j.jhydrol.2016.05.033.

Peruccacci, S. *et al.* (2017) 'Rainfall thresholds for possible landslide occurrence in Italy', *Geomorphology*. Elsevier, 290(January), pp. 39–57. doi: 10.1016/j.geomorph.2017.03.031.

Rodriguez, F., Bocher, E. and Chancibault, K. (2013) 'Terrain representation impact on periurban catchment morphological properties', *Journal of Hydrology*, 485, pp. 54–67. doi: 10.1016/j.jhydrol.2012.11.023.

Rotterdam open data store (2018).

Schellart, A. N. A., Shepherd, W. J. and Saul, A. J. (2012) 'Influence of rainfall estimation error and spatial variability on sewer flow prediction at a small urban scale', *Advances in Water Resources*. Elsevier Ltd, 45, pp. 65–75. doi: 10.1016/j.advwatres.2011.10.012.

Schleiss, M. (2016) 'A Geostatistical Framework for Quantifying the Temporal Evolution and Predictability of Rainfall Fields', *Journal of Hydrometeorology*, 17(3), pp. 915–929. doi: 10.1175/JHM-D-15-0137.1.

Schuurmans, W. and Leeuwen, E. Van (2017) '3Di : A new Dutch hydrological model'.

Segond, M. L., Wheater, H. S. and Onof, C. (2007) 'The significance of spatial rainfall representation for flood runoff estimation: A numerical evaluation based on the Lee catchment, UK', *Journal of Hydrology*, 347(1–2), pp. 116–131. doi: 10.1016/j.jhydrol.2007.09.040.

Shi, P. J. *et al.* (2007) 'The effect of land use/cover change on surface runoff in Shenzhen region, China', *Catena*, 69(1), pp. 31–35. doi: 10.1016/j.catena.2006.04.015.

Sriwongsitanon, N. and Taesombat, W. (2011) 'Effects of land cover on runoff coefficient', *Journal of Hydrology*. Elsevier B.V., 410(3–4), pp. 226–238. doi: 10.1016/j.jhydrol.2011.09.021.

Statline - Statistics Netherlands (2017). Available at: http://statline.cbs.nl/StatWeb/publication/?DM=SLNL&PA=37230NED&D1=17-18&D2=57-650&D3=l&LA=EN&HDR=T&STB=G1,G2&VW=T (Accessed: 10 January 2018).

Storm Water Management Shiawassee County (2015) *MDOT Drainage Manual - Table 3-1 Runoff Coefficients for Rational Formula*.

Sun, X. *et al.* (2000) 'Flood estimation using radar and raingauge data', *Journal of Hydrology*, 239(1–4), pp. 4–18. doi: 10.1016/S0022-1694(00)00350-4.

Ten Veldhuis, J. A. E. and Olsen, A. S. (2012) 'HYDROLOGICAL RESPONSE TIMES IN LOWLAND URBAN CATCHMENTS CHARACTERISED BY LOOPED DRAINAGE SYSTEMS by', (December), pp. 290–294.

Waterschap Hollandse Delta (2013) *Rioolvreemd water rioolwaterzuiveringsinrichting Dokhaven*.

Weather TU Delft (2018). Available at: http://weather.tudelft.nl/csv/ (Accessed: 14 January 2018).

Yin, H. *et al.* (2017) 'Determination of urban runoff coefficient using time series inverse modeling', *Journal of Hydrodynamics, Ser. B*. Publishing House for Journal of Hydrodynamics, 29(5), pp. 898–901. doi: 10.1016/S1001-6058(16)60803-X.

Young, C. B., McEnroe, B. M. and Rome, A. C. (2009) 'Empirical Determination of Rational Method Runoff Coefficients', *Journal of Hydrologic Engineering*, 14(12), pp. 1283–1289. doi: 10.1061/(ASCE)HE.1943-5584.0000114.

7. Appendix

7.1 Rainfall input

Table 15: Rainfall input of district 5 for all events and all resolutions [m³]

Event	00	01	02	03	04	05	06	07	08	09	10
A1	9336	9400	15235	7563	9316	15170	11281	9640	10066	13267	9613
A2	8765	9430	12933	7837	9288	15014	11074	9663	9884	12825	9783
A3	9858	9260	18944	7016	9841	14632	11597	9585	9483	13204	9607
A5	8957	7801	10417	7618	7648	15613	9540	10337	11775	14311	8837
A10	8143	8451	8990	7428	6318	16711	10638	9982	10940	12759	9736
B1	10985	11051	17912	8896	10964	17856	13271	11343	11845	15618	11305
B2	10328	11086	15279	9210	10936	17673	13032	11368	11632	15109	11501
B3	11595	10896	22299	8257	11590	17223	13637	11274	11161	15534	11303
B5	10537	9177	12255	8963	8997	18368	11223	12160	13852	16836	10396
B10	9580	9942	10576	8738	7433	19660	12515	11743	12870	15011	11454
C1	16208	16333	26467	13136	16166	26323	19589	16734	17472	23015	16698
C2	15186	16388	22330	13627	16107	26048	19221	16778	17151	22228	17002
C3	17119	16073	32870	12179	17066	25387	20146	16643	16456	22925	16680
C5	15551	13544	18086	13227	13279	27108	16563	17947	20444	24847	15343
C10	14138	14673	15609	12897	10970	29015	18471	17331	18994	22153	16904

Table 16: Rainfall input of district 30 for all events and all resolutions [m³]

Event	00	01	02	03	04	05	06	07	08	09	10
A1	27382	25953	28552	27553	19696	40590	25066	22691	19007	34852	34628
A2	29947	24490	24859	28323	18657	41024	19858	19097	17262	35893	33468
A3	29414	24425	24243	27754	18756	40844	20286	19134	17296	35553	33211
A5	27149	25140	29713	30157	17768	37881	22015	20801	18290	38233	31971
A10	30944	25072	51275	22950	19050	38827	31892	27225	24554	42682	30290
B1	36390	34595	37822	36542	26074	53931	33359	30357	25249	46394	46193
B2	39946	32467	32925	37606	24771	54680	25897	25180	22795	47722	44493
B3	39418	32533	31770	36921	25047	54519	26921	25368	22876	47210	44393
B5	36297	33647	39727	40268	23803	50497	29604	27960	24558	50788	42753
B10	41162	33351	68207	30528	25340	51647	42422	36215	32662	56776	40293
C1	68237	64019	68716	67795	48550	100409	61809	55858	46651	86226	85783
C2	74403	60225	60804	69758	46034	101773	47820	46578	42206	88617	82702
C3	73495	60370	58183	68595	46582	101486	49687	46872	42261	87685	82640
C5	67480	62555	73855	74857	44255	93862	55054	51994	45665	94387	79482
C10	76502	61985	126768	56739	47097	95991	78845	67308	60705	105523	74887

Table 17: Rainfall input of district 36 (incl. 29) for all events and all resolutions [m³]

Event	00	01	02	03	04	05	06	07	08	09	10
A1	71216	63245	78579	71205	44327	96431	55973	50862	45859	95902	79090
A2	70520	60455	68593	72343	42735	95863	50096	46133	43403	95237	77786
A3	71092	60430	75966	67324	38862	93797	53528	43230	41664	95862	76165
A5	57732	51552	63118	67028	35167	88957	37295	35932	33061	99695	67523
A10	77550	62834	128503	57516	47742	97305	79925	68229	61536	106968	75912
B1	83397	73677	87912	84503	51809	113554	63288	57238	52705	112451	92196
B2	82216	69840	76429	84804	49582	112759	56268	51755	49685	111328	90484
B3	83359	70026	85214	79092	45647	110631	60460	49522	48067	112563	89366
B5	67191	59840	73455	78252	40712	104230	42615	41131	37994	117557	78548
B10	91232	73920	151175	67664	56165	114472	94026	80267	72393	125840	89305
C1	131936	124780	133697	130331	90045	190645	114158	109076	89613	169857	165541
C2	132652	112223	120712	136759	80363	182918	89319	83081	79810	179280	146508
C3	134147	111999	132948	127879	74067	179405	94872	78999	76966	181454	144303
C5	108160	96223	118239	126120	65394	168237	68083	65760	60844	190229	126415
C10	147493	119505	244403	109391	90801	185066	152010	129766	117037	203445	144379

7.2 Comparison of rainfall volumes of the weather stations and the radar per event and district

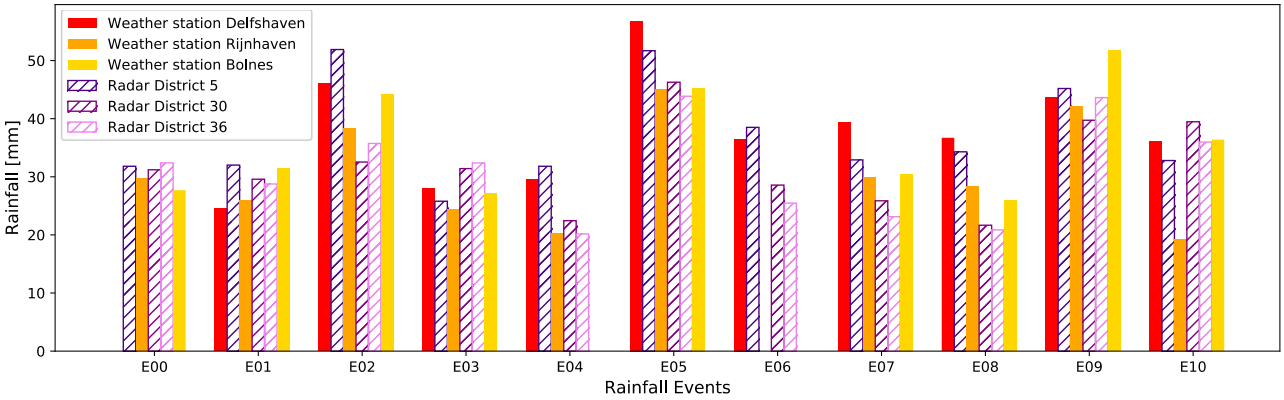

7.3 Boxplots of the normalized water balances per resolution combination

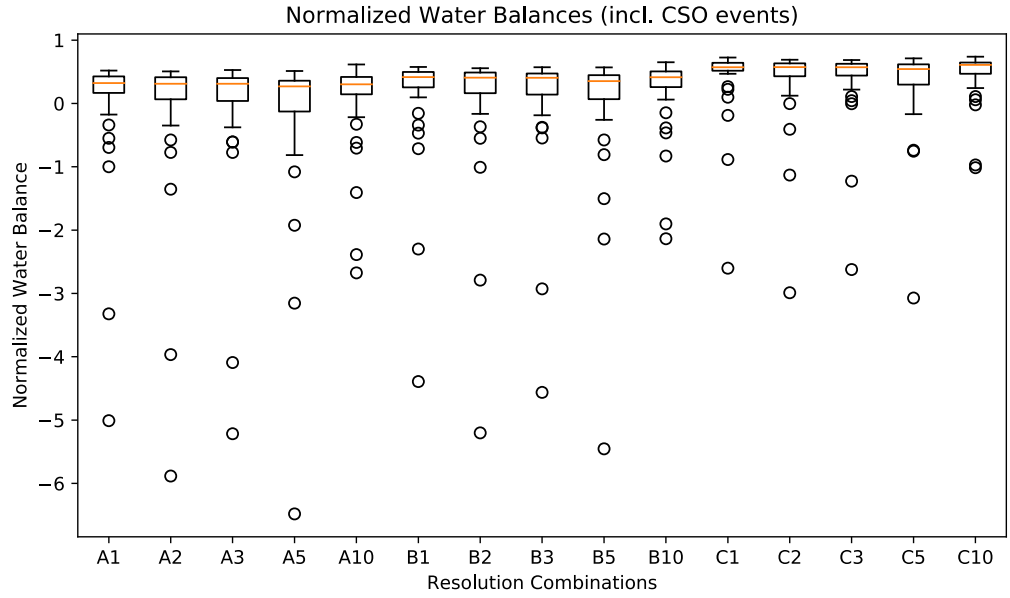

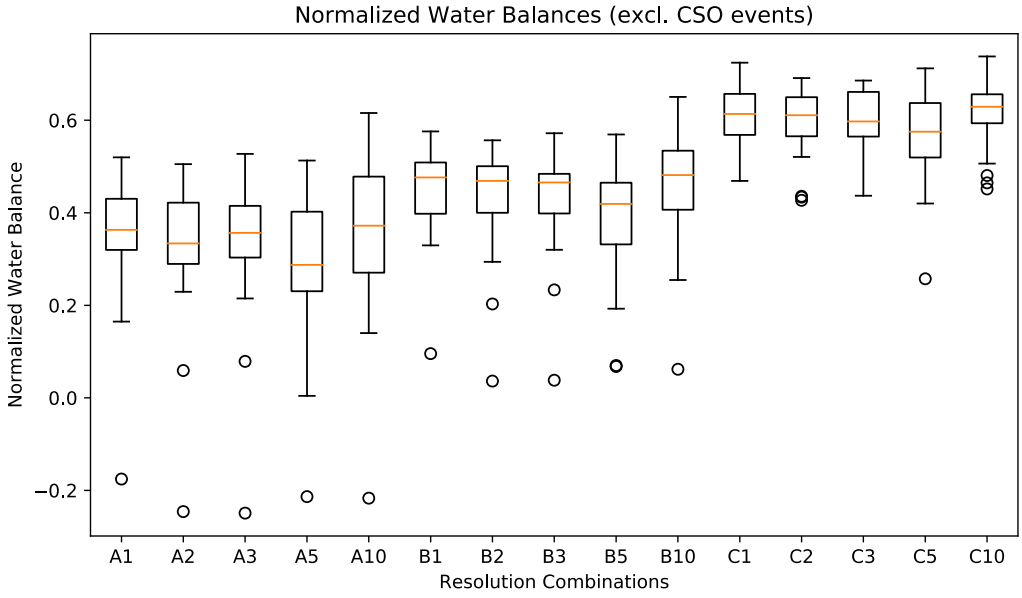

7.4 Resolution-specific normalized water balances per district and event